

A helium nanodrop bouncing off a wall

This article has been downloaded from IOPscience. Please scroll down to see the full text article.

2004 J. Phys. A: Math. Gen. 37 2781

(<http://iopscience.iop.org/0305-4470/37/7/019>)

View [the table of contents for this issue](#), or go to the [journal homepage](#) for more

Download details:

IP Address: 171.66.16.66

The article was downloaded on 02/06/2010 at 19:59

Please note that [terms and conditions apply](#).

A helium nanodrop bouncing off a wall

G Kälbermann

Soil and Water Department, Faculty of Agriculture, Rehovot 76100, Israel

E-mail: hope@vms.huji.ac.il

Received 28 July 2003

Published 4 February 2004

Online at stacks.iop.org/JPhysA/37/2781 (DOI: 10.1088/0305-4470/37/7/019)

Abstract

We depict the quantum collision between a stable helium nanodrop and an infinitely hard wall in one dimension. The scattering outcome is compared to the same event omitting the quantum pressure. Only the quantum process reflects the effect of diffraction of wave packets in space and time.

PACS numbers: 03.65.Nk, 31.15.Ew, 42.25.Fx, 67.20.+k

1. Introduction

In recent years we have described the effect named *diffraction of wave packets in space and time*. The effect consists of a multiple peak wave train that is generated in a scattering event by the interference between the incoming and the scattered packets. The wave train lasts to infinite time, due to the spreading of the incoming packet, which catches up with the scattered packet [1–6].

The effect occurs in matter wave scattering. It persists only for narrow enough packets compared to the scatterer extent. The effect was demonstrated numerically and analytically in various settings. As a possible laboratory experiment to verify the effect experimentally we suggested a collision between a helium drop and a reflecting wall [3]. In [3] we omitted completely the self-interaction of the drop. The impinging packet that statistically represented the behaviour of the drop was taken as a Gaussian packet, for which we could provide exact analytical expressions. However, the self-interaction provides the binding energy of the drop and hinders spreading, which is crucial for the appearance of the diffraction pattern. A more realistic calculation was needed.

Helium is a relatively weakly bound liquid, even close to 0 K. It is weaker than liquid water or other liquids at ambient temperature. The binding energy per ^4He atom in the superfluid phase is around $E_b = -7.5$ K [8] whereas for liquid water it is around -5500 K, depending on the temperature and pressure.

The helium atoms are neutral and do not benefit from strong hydrogen-like bonds for their binding. The apparent weakness of the interactions is nevertheless misleading. A helium drop interacts with itself in a much stronger manner than a Bose–Einstein condensate (BEC)

[7], and even there the nonlinear effects of the self-interaction are important. In particular the interatomic forces dominate the so-called quantum pressure or quantum potential in the bulk of the drop. Inside the drop the density is constant and the quantum pressure vanishes. Near the edge of a drop, curvature effects take over and the quantum pressure becomes relevant.

In the present work we investigate numerically the quantum scattering of a helium droplet bouncing off an infinitely hard wall. The aim is twofold: firstly an investigation like the present has never been carried out before and it is interesting in its own merit and, secondly we would like to have a more realistic treatment of the diffraction of wave packet effect in the context of liquid helium.

In order to simplify the treatment as much as possible we resort to the *density functional* approach.

Density functional theories resort to the solution of a one-body nonlinear Schrödinger equation for a particle of mass m ,

$$i\frac{\partial\psi}{\partial t} = -\frac{1}{2m}\vec{\nabla}^2\psi + [O(|\psi|^2) + U(\vec{r})]\psi \quad (1)$$

where $O(|\psi|^2)$ is a nonlinear and sometimes nonlocal [8] functional of the density $\rho = |\psi|^2$, and $U(\vec{r})$ an external potential. The commonly used mean-field equation for BEC systems belongs to this class of equations [7]. In this case it is referred to as the Gross–Pitaevskii equation.

Density functional theory has been extremely successful in reproducing the properties of helium nanodroplets [8]. Besides the mean binding energy per particle, average density, incompressibility and surface tension at zero temperature both for ^4He and ^3He , in a stationary state [9], it accounts for capillary effects at low temperatures [10], the phase diagram of liquid–vapour coexistence [11], as well as the excitation spectrum (phonon–maxon–roton) of liquid helium [8]. The model has been verified experimentally in scattering reactions [12]. It is currently being applied to other areas of superfluid dynamics such as electron bubbles [13], adsorption on plates of alkali metals [14], vortex line pinning [15], etc.

The density functional theory is therefore a respectable method for the treatment of helium nanodroplet scattering. In the next section we present results for the scattering of helium nanodroplets in one dimension with and without the quantum potential. The last section provides some comments emerging from the observation of the numerical data.

2. A helium drop colliding with a wall

A nonlinear, local, self-interaction of the helium drop was proposed some time ago by Stringari and Treiner [9]. The parameters of the density functional were fitted to the known values of the binding energy per atom in the bulk, the incompressibility, the infinite atom–matter density and the surface tension. Improvements to this functional seem to require nonlocal terms [7]. Such terms are engineered to reproduce the excitation spectrum of liquid helium below the λ transition point in a more accurate manner. In the present work we opt for the local version that is more manageable computationally and still quite successful phenomenologically.

The operator $O(\rho)$ of equation (1) is given by

$$O(\rho) = b\rho + \frac{c}{4}(4 + 2\gamma)\rho^{1+\gamma} - 2d\vec{\nabla}^2\rho \quad (2)$$

with $b = -888.81 \text{ K \AA}$, $c = 1.045\,54\,10^7 \text{ K \AA}^{3+3\gamma}$, $\gamma = 2.8$, $d = 2383 \text{ K \AA}^5$.

For the one-dimensional case treated presently we use the same parameter set, assuming independence from the y , z directions, i.e. an infinite planar slab.

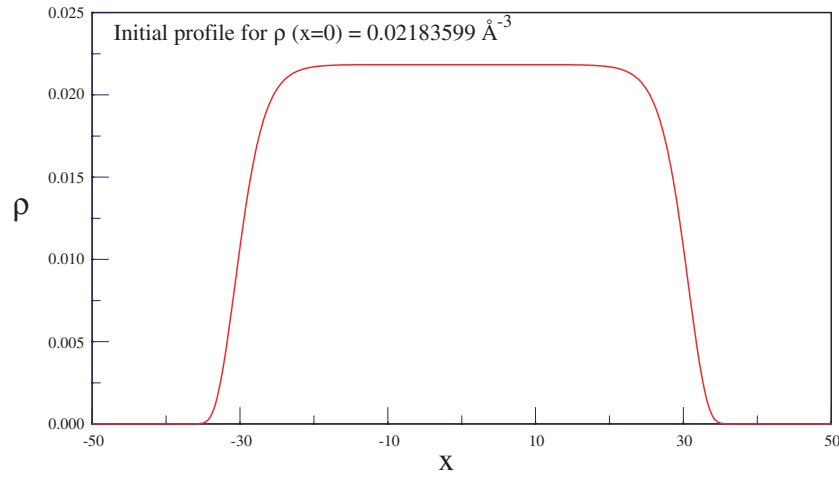


Figure 1. Density profile of a helium drop in \AA^{-3} for $\rho(x=0) = 0.02183599 \text{\AA}^{-3}$ as a function of distance in \AA .

The stationary solutions of equation (1) with the self-interaction of equation (2), in one spatial dimension are obtained from the substitution $\Psi(x, t) = e^{i\mu t} \phi(x)$, with μ being the chemical potential. For finite size drops, μ is a parameter, whose value determines the number of particles in the drop and tends to the bulk binding energy when the number of particles tends to infinity. For ^4He , it is $\mu_\infty = -7.15 \text{ K}$.¹

Stationary solutions are found by integrating the equation [9]

$$\mu = b\rho + \frac{2+\gamma}{2} c\rho^{1+\gamma} - \left(2d + \frac{1}{4m\rho}\right) \frac{d^2\rho}{dx^2} + \frac{\left(\frac{d\rho}{dx}\right)^2}{8m\rho^2} \quad (3)$$

or equivalently

$$\left(\frac{d\rho}{dx}\right)^2 = \frac{8m\rho}{8m\rho d + 1} \left(-\mu\rho + \frac{b\rho^2}{2} + \frac{c\rho^{2+\gamma}}{2}\right). \quad (4)$$

The integration of equation (4), proceeds by a choice of $\rho(x=0) < \rho(x=0)_\infty = 0.021836 \text{\AA}^{-3}$, the bulk helium liquid density for atomic matter. Equation (4), with $\frac{d\rho}{dx}|_{x=0} = 0$, fixes the value of the chemical potential $\mu > \mu_\infty$. The numerical roundoff error limits the possibilities of approaching $\rho(x=0)_\infty$ closer than 10^{-7} and still obtain a profile density that decays at infinite distances. We therefore chose the closest value we could and used this profile density in all the scattering events to be presented below. The parameter for this density profile is $\rho(x=0) = 0.02183599$, which yields $\mu = -6.71 \text{ K}$. The number of particles per unit area

$$N = \int_{-\infty}^{\infty} dx \rho(x) \quad (5)$$

for this case is $N = 1.288 \text{\AA}^{-2}$, or an effective length $X_{\text{eff}} = N/\rho(x=0) = 59 \text{\AA}$. The drop then extends some 59\AA along the x axis and is infinite along the y, z plane. The solution in the three-dimensional case is not much different; in this case, the drop contains around 4500 atoms. Figure 1 shows this initial density profile.

¹ The transformation to standard energy units proceeds by multiplication with Boltzmann's constant k .

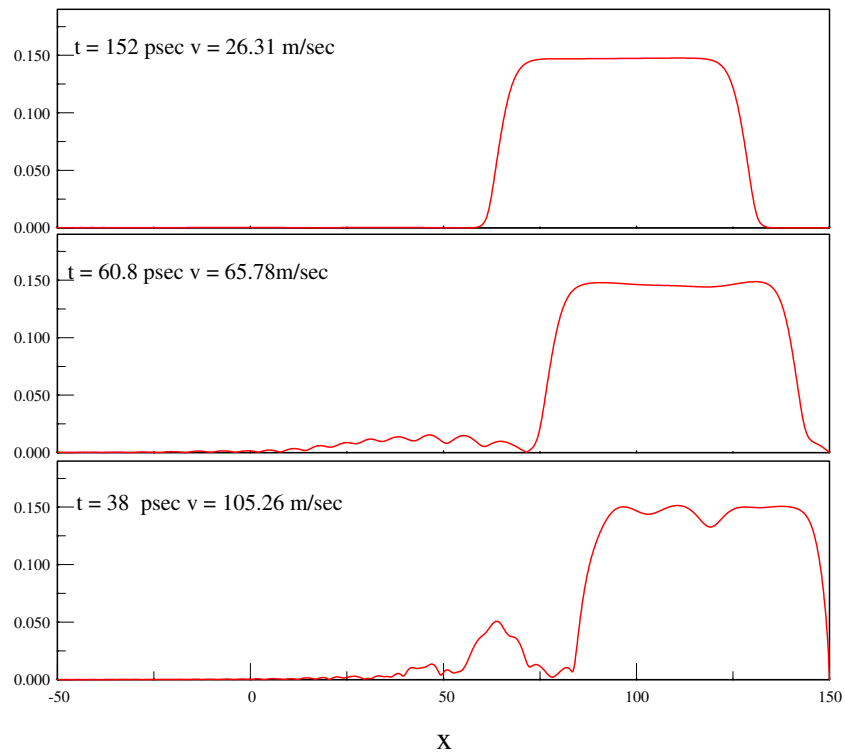


Figure 2. $|\Psi|$ as a function of distance in units of Å for various velocities and times.

The details of the scattering are not very sensitive to the number of particles and the extension of the drop. The majority of the particles reside within the bulk. The diffraction effects depend on the side wings of the distribution in figure 1 and are therefore almost the same for any number of particles, because the width of these wings is determined by the parameters of the nonlinear potential only.

In the next section we will show results for smaller size drops whose profile resembles a Gaussian. For such drops the interference effect is cleaner, but not qualitatively different.

The scattering starts with a drop impinging from the left onto an infinitely hard wall located to the far right. We took a drop centred at $x_0 = 110$ Å with velocity v , defined by

$$\psi(x, t = 0) = e^{imv(x-x_0)} \sqrt{\rho(x)}. \quad (6)$$

The wall is located at $x = 150$ Å. We use a five-step predictor corrector method [13] for the numerical integration. We demand an accuracy of more than 0.1% in both the conservation of normalization of the wave and the energy. This strict demand requires a tiny time step of around 10^{-17} s, and consequently lengthy runs of around 10^7 iterations. A larger time step causes rapid deterioration of the accuracy and runaway behaviour. A tiny time step is needed, due to the large values of the constants entering the self-interaction.

It was found that for packet velocities below around $v = 50$ m s $^{-1}$ the drop collides with the wall elastically with a barely noticeable distortion. Such a threshold corresponds to a momentum transfer per particle at the wall of the order of $\Delta p = 2mv \approx 0.62$ Å $^{-1}$. This is a typical value for the excitation of ripplons at the surface of a drop [16].

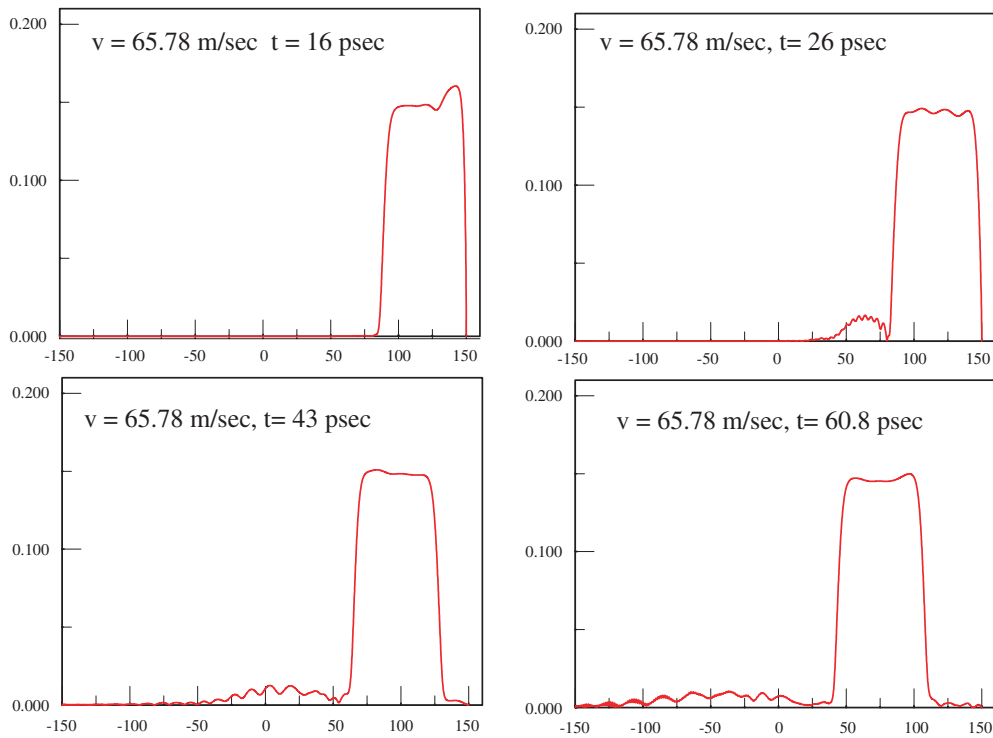


Figure 3. Time snapshots of $|\Psi|$ as a function of distance in units of \AA for $v = 65.78 \text{ m s}^{-1}$.

The drop travels without strictures, hence there is no superfluid limiting velocity, and it can remain superfluid up to any velocity; in practice the drop flows over a surface that limits the maximum frictionless speed. The experiment may also be viewed as the one in which the wall is moved crashing into the stationary drop. We have performed such calculations in order to check our numerical schemes, and found them to agree with the results of a moving packet and a fixed wall as expected.

Figure 2 exemplifies the result of the scattering for various velocities and times, such that $\Delta x = vt$, for all of them is the same in the free case. Above the threshold velocity there appears a multiple peak structure that recedes faster than the packet. It resembles the diffraction in space and time structures given in [1–6]. For high enough velocities, the collision is inelastic. The energy is transferred to waves that recede faster than the bulk of the drop. The drop is almost stalled at the wall. In the bottom graph of figure 2, the collision process is still under way and the multiple peak structures are still being generated. There is a background hump under the peaks in the middle graph. This elevation is an incoherent background, similar to that occurring in the *diffraction in space and time phenomenon* [1–6] for wide packets. In the next section we show graphs for a thinner drop, for which the background is almost absent.

Figure 3 shows the evolution of the scattering process for a velocity of $v = 65.78 \text{ m s}^{-1}$.²

The density fluctuations inside the packet due to the collision are progressively expelled out of the drop. This multiple peak tail wave, is a product of both the incoming and the reflected waves interfering with each other.

In order to confirm the hypothesis that the interference effects are responsible for the multiple peak structures, we performed parallel calculations for the analogous classical drop,

² The awkward value of the velocity originates from a convenient choice of time units.

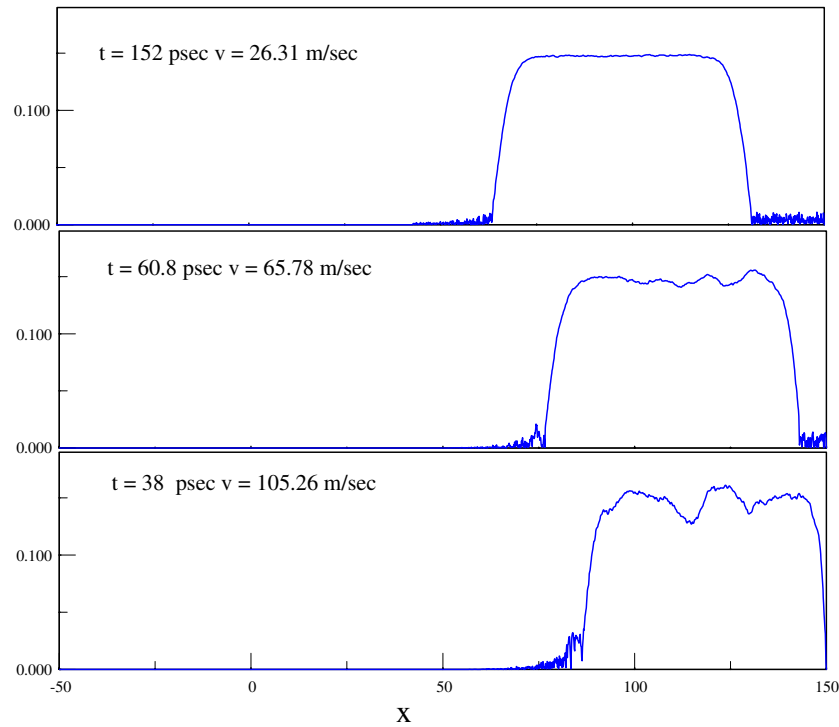


Figure 4. $|\Psi|$ as a function of distance in units of Å for various velocities and times for the classical case.

by subtracting the quantum potential in the Schrödinger equation. In equation (1) $O(\rho)$ is replaced by $O(\rho) - U_{\text{quantum}}$, with

$$U_{\text{quantum}} = -\frac{1}{2m\sqrt{\rho}} \frac{d^2\sqrt{\rho}}{dx^2}.$$

For the classical scattering case, we use the same initial profile as that depicted in figure 1, although it is not a stationary solution with the quantum potential subtracted. As a matter of fact there are no stationary solutions without the quantum potential. This may be easily seen by expanding around the vacuum.

Such an expansion produces the equation

$$\frac{d^2\rho}{dx^2} = \frac{b}{2d}\rho \quad (7)$$

whose solutions are oscillatory, with the density becoming eventually negative.

Figure 4 depicts the classical scattering graphs corresponding to the quantum events of figure 2. As is evident from the figure, the classical collision does not produce a multiple peak tail. The collision results in large density fluctuations in the bulk and noisy fluctuations at the edges.

The corresponding classical packet evolution for $v = 65.78 \text{ m s}^{-1}$ is shown in figure 5.

The quantum scattering resists distortions in the bulk and gets rid of the energy in the form of coherent wave trains, whereas the classical scattering that lacks the quantum potential curvature-like term, renders the packet softer to deformations. The coherence of the tail region is visualized in figure 6. The classical scattering phase at the bottom is coherent inside the

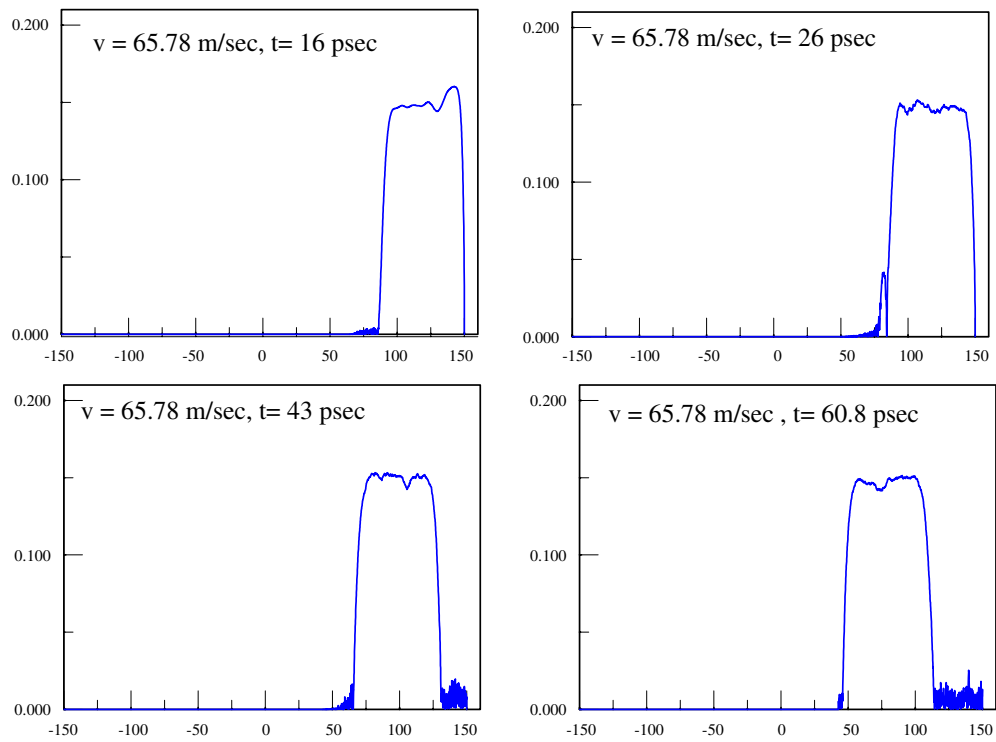


Figure 5. Time snapshots of $|\Psi|$ as a function of distance in units of \AA for $v = 65.78 \text{ m s}^{-1}$ for the classical case.

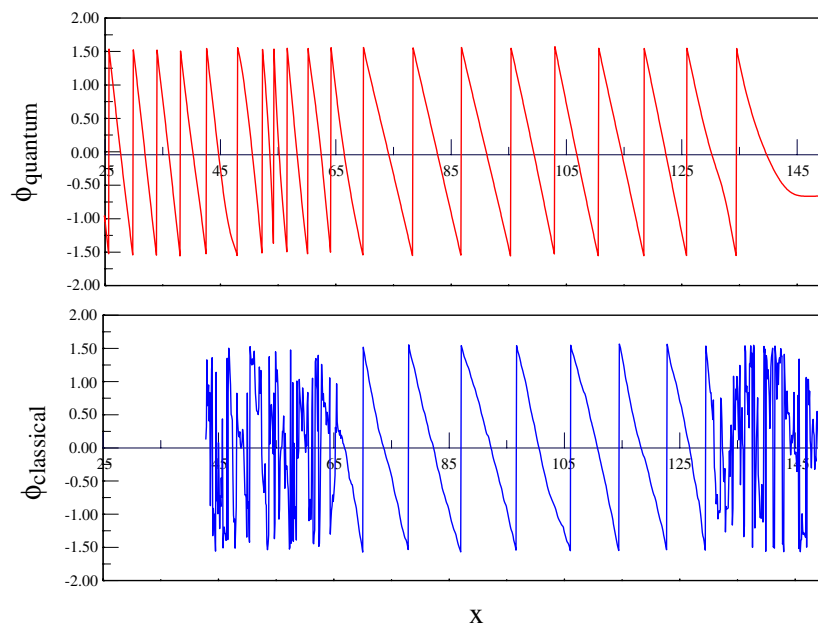


Figure 6. Wave function phase $\phi = \tan^{-1}[\frac{\text{Im}(\Psi)}{\text{Re}(\Psi)}]$, for the quantum and classical cases, as a function of distance in units of \AA , $v = 65.78 \text{ m s}^{-1}$.

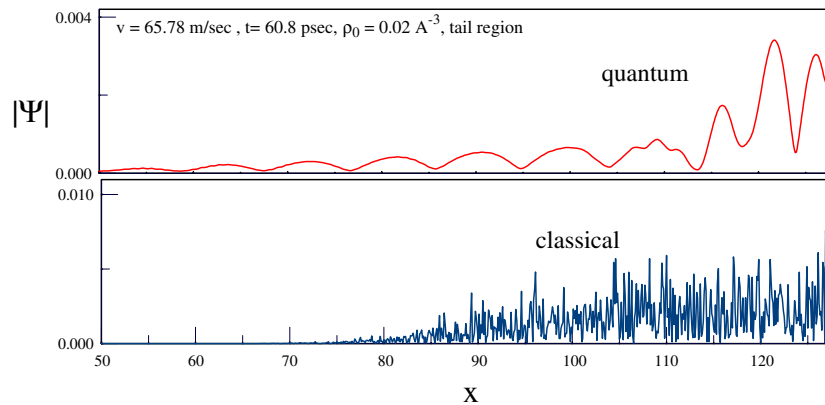


Figure 7. Quantum versus classical scattering for $v = 65.78 \text{ m s}^{-1}$, $\rho(x = 0) = 0.02 \text{ \AA}^{-3}$, enlargement of tail region. $|\Psi|$ as a function of distance in units of \AA .

drop corresponding to a travelling packet of fixed velocity, and incoherent or even random at the surface. The quantum phase is coherent both inside and outside (only part of the outside region is shown). The wavelength outside the bulk of the drop in the upper graph, for $x < 70 \text{ \AA}$ is smaller than the wavelength in the bulk. The multiple peak tail recedes faster than the drop.

3. Conclusions

We have provided snapshots illustrating the behaviour of a helium nanodrop treated by means of the density functional approach, in a collision event with a hard wall. The numerical results confirm that the effect of *diffraction of wave packets in space and time* does express itself in ^4He nanodrop scattering. The results for a thick drop presented in the last section are not as clean as those of [3]. A thick drop has a sizeable self-interaction and tends to conserve its shape in the collision. To enhance the effect, we also considered smaller size drops. Using $\rho(x = 0) = 0.02 \text{ \AA}^{-3}$, the number of particles per unit area is now $N = 0.26 \text{ \AA}^{-2}$, and the effective extent is $X_{\text{eff}} = 12.5 \text{ \AA}$. A three-dimensional drop of this type contains around 40 atoms.

Figure 7 depicts the classical and quantum scattering results for a velocity of $v = 65.78 \text{ m s}^{-1}$ at $t = 60.8 \text{ ps}$ in the tail region. The asymptotic behaviour of the quantum event is much cleaner than that of the thicker drop depicted in the previous section.

The existence of a diffraction tail is expected for the collision of a quantum packet with a barrier [1–6]. The present work shows that, even for self-interacting quantum systems, such as a helium nanodrop, the effect persists, being more marked the smaller the number of particles in the packet. In summary, it appears that it could be possible to observe the diffraction phenomenon described in [1–6] with ^4He nanodrops by colliding them with a hard surface at high enough speed.

References

- [1] Kälbermann G 1999 *Phys. Rev. A* **60** 2573
- [2] Kälbermann G 2001 *J. Phys. A: Math. Gen.* **34** 3841
- [3] Kälbermann G 2001 *J. Phys. A: Math. Gen.* **34** 6465
- [4] Kälbermann G 2002 *J. Phys. A: Math. Gen.* **35** 1045

-
- [5] Kälbermann G 2002 *J. Phys. A: Math. Gen.* **35** 4599
 - [6] Kälbermann G 2002 *J. Phys. A: Math. Gen.* **35** 9829
 - [7] Dalfovo F, Giorgini S, Pitaevskii L P and Stringari S 1999 *Rev. Mod. Phys.* **71** 463
 - [8] Dalfovo F, Pricauptenko L, Stringari S and Treiner J 1995 *Phys. Rev. B* **52** 1193
 - [9] Stringari S and Treiner J 1987 *Phys. Rev. B* **36** 8369
 - [10] Calbi M M, Toigo F, Gatica S and Cole M W 1999 *Phys. Rev. B* **60** 14935
 - [11] Biben T and Frenkel D 2002 *J. Phys.: Condens. Matter* **14** 9077
 - [12] Harms J, Toennies P and Dalfovo F 1998 *Phys. Rev. B* **58** 3341
 - [13] Eloranta J and Apkarian V A 2002 *J. Chem. Phys.* **117** 10139
 - [14] Szybisz L 2003 *Phys. Rev. B* **67** 132505
 - [15] Barranco M, Mayol R, Pi M M and Dalfovo F 2002 *J. Low Temp. Phys.* **126** 281
 - [16] Ebner C and Saam W F 1975 *Phys. Rev. B* **12** 923